Int. J. Thermal-Fluid Engineering and Modern Energetics 1 (2022) 19-33 www.tfeme-ba.com
doi: 10.51558/2831-0527.2022.1.1.19

Article

Experimental and Artificial Neural Network Investigation on the Thermal Efficiency of Two-Phase Closed Thermosyphon

Engin Gedik*[1], Hüseyin Kurt[2], Murat Pala[3], Abdulla Alakour[4], Metin Kaya[1]

[1] *Energy Systems Engineering Department, Technology Faculty, Karabuk University, Karabuk, Turkey*
[2] *Mechanical Engineering Department, Engineering Faculty, Necmettin Erbakan University, Konya, Turkey*
[3] *Civil Engineering Department, Engineering Faculty, Adıyaman University, Adıyaman, Turkey*
[4] *Energy Systems Engineering Department, Institute of Graduate Programs, Karabuk University, Karabuk, Turkey*

*Corresponding author institutional e-mail address (egedik@karabuk.edu.tr)

A R T I C L E I N F O

Article history:

Available online 1 July 2022

Keywords:

Thermal efficiency
Heat pipe
Two-phase closed thermosyphon
ANN

A B S T R A C T

The main purpose of this study is to investigate the thermal efficiency of a Two-Phase Closed Thermosyphon (TPCT). For this purpose, initially, an experimental study was performed, then to predict the other experimental conditions ANN model which has used a wide range of thermal engineering systems was developed. A vertical copper pipe charged with different working fluids as pure water, ethanol, and ethylene glycol were used for TPCT. Impact of the various parameter such as heating power input, inclination angle, cooling water flow rate and working fluid type on the TPCT efficiency are examined. It is found that the increase in the inclination angle increased the TPCT efficiency while the increase in heating power input decreased efficiency. Regression analysis was applied to examine the performance of ANN between estimated and experimental data. The Mean Absolute Percentage Error (MAPE) was found to be less than 1.3 % for the training set and 3.1% for the test data set. The ANN predictions yield R2 in the range of 0.9998 for the training set and 0.9989 for the test data set. The obtained results from the experimental study and ANN were found in good agreement, and it is also concluded that from the study the ANN is a useful tool to estimate such thermal engineering problems.

1. Introduction

TPCTs which are a superior heat transfer device is an important issue for applications in a wide range of thermal engineering systems (Gedik, 2016 [1]; Gedik et al., 2016 [2]; Andrzejczyk, 2019 [3]; Sarafraz et al., 2020 [4]). Thermosyphons consist of three different regions: i) evaporator (the working fluids absorb heat from outside), ii) condenser (the heat transferred to the external environment), and iii) is the adiabatic section where heat transfer does not occur. The schematic illustration and working principle of TPCT are given in Figure 1. The heat energy that is executed to the evaporator region of the TPCT causes the working fluid to vaporize. Using absorbed heat from the condenser region of the TPCT, working fluid that becomes to be saturated vapor condenses and turns back to the evaporator region of the device in various ways. To send the fluid, which is condensed in the condenser region, back to the evaporator region can benefit from gravity, centrifugal, magnetic, and electrostatic forces. To organize a working fluid cycle inside the TPCT, a wick made from suitable materials is placed inside the inner surface of the TPCT.

In general, because the evaporator region is placed at the low position of the TPCT, the cycle can be provided easily by making use of gravity without needing any extra force. The most general ways to take the condensed fluid back to the evaporator region are gravity and capillary actions (Faghri, 1995 [5]; Fadhl et al., 2013 [6]; Kerrigan et al. [7], Fadhl et al., 2015 [8]).

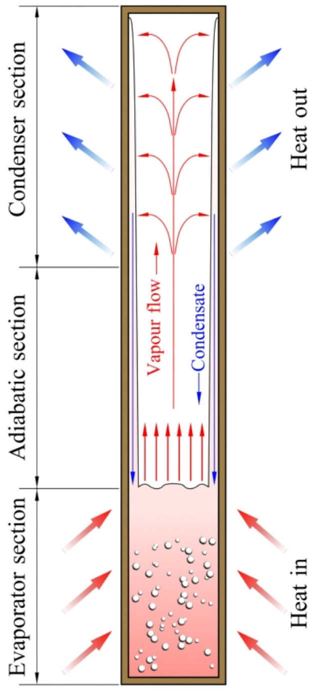

Figure 1. Schematical illustration and working principle of TPCT.

Many studies (Farsi et al., 2003 [9]; Kamyar et. al., 2013 [10]; Jafari et. al., 2016 [11]; Jafari et al., 2017 [12]; Ma et al., 2017 [13]; Naresh & Balaji, 2018 [14]) have previously reported an increase in heat transfer via thermosyphon taking into account the type of working fluids (Huminic & Huminic 2011[15]; Kannan et al., 2014 [16]) angle of the TPCT (Noie et al., 2007 [17]) filling ratio (Ong et al., 1999 [18]; Park et al., 2002 [19]; Shabgard et al., 2014 [20]) of working fluid etc. One of them was performed by Payakuruk et al., (2000) [21]. In their study heat transfer characteristics of TPCT were investigated from the point of view of various parameters configuration of inclination angle and working fluids. Fadhl et al. (2015) [8] investigated numerically TPCT by using the CFD method. Their CFD results showed close agreement with the previously published experimental results. Gedik et al., (2016) [2] have studied TPCT integrated with heat recovery system to investigate its thermal performance. They have used the R134a and R410A working fluids with an effectiveness of 35.6% and 57.7% respectively inside the TPCT. According to them, in heat recovery applications, the usage of a heat pipe bundle system is beneficial. Sözen et al., (2016) [22] experimentally investigated the fly ash effect on the thermal performance of TPCT. Three kinds of metal oxide nanoparticles suspended in water were used in the thermosyphon as a working fluid and its thermal performance was studied for various test configurations such as heating powers, coolant water flow rates, etc. They found that a meaningful decrease in thermal resistance of thermosyphon when used nanofluid containing fly-ash inside the thermosyphon.

The ANN is a method that can be applied successfully in many engineering fields to expand and predict experimental results (Boostani et al., 2017 [23]). This method has many more advantages such as simplicity, high speed, nonlinear modeling when compared to classical methods (Kalogirou, 2001 [24]; Kurt et al., 2006 [25]; Kurt &Kayfeci, 2009 [26]). It has several models as described by Sarle, (1994) [27]. In addition, it can be seen in many studies that ANN gives more accurate results than linear models (Chaloulakou, 2003 [28]) and it is used successfully in the examination of engineering systems (Fichera & Pagano, 2002 [29]; Sanaye & Hajabdollahi, 2010 [30]; Caner et al., 2011[31]; Ceylan et al., 2014 [32]). Akdağ et al., (2009) [33] studied ANN to predict the heat transfer in oscillating circular flow generated by a piston-cylinder mechanism. They found that a good agreement between experimental and ANN results; additionally, they concluded that ANN is a useful tool to model the heat transfer. Shanbedi et al. (2015) [34] have used the Adaptive Neuro-Fuzzy Inference System to predict the thermal performance of TPCT. Results obtained from their study showed that the studied model is susceptible and reliable to optimize TPCT performance. In order to predict the experimental results for the thermal performance of TPCT filled with nanofluids, the ANN model was used by Shanbedi et al., (2013) [35]. Komeilibirjandi et al., (2020) [36] used correlations and ANN model to forecast the thermal conductivity of CuO/water nanofluids. Filing ratio and different heat input effect on the thermosyphon performance was investigated by Sadrameli et al., (2020) [37]. It is found that the efficiency of TPCT at different levels of heat input was between 73 and 78%. Heat transfer characteristics of copper-coated and uncoated wickless heat pipe (namely TPCT) filled with R134a working fluid have been experimentally studied by Senthilkumar et. al., (2020) [38]. They found that coated wickless heat pipe is more efficient than uncoated heat pipe for 10 kWm-2 and at inclination angle of TPCT 45°.

Based on the above literature studies and according to the best of authors' knowledge, although there are many papers on two-phase closed thermosyphon considered various operation conditions, far less work has been considered using ANN method for TPCT despite its reliability, accuracy in many engineering systems. Therefore, according to the authors, the study is considerable. For this reason; the motivation and objective of this study is to examine the thermal efficiency of TPCT utilizing ANN method evaluation. For this purpose, careful experimental tests were performed taking into consideration various operation conditions such as inclination angle of TPCT, working fluids, heating power input and cooling flow rate. To predict the rest of experimental conditions, ANN model was developed. In ANN model, the backpropagation learning algorithm was used to be able to train the network. The obtained results from the study were plotted graphically and discussed in detail.

2. Methodology

2.1. Experimental Study

The schematic illustration of the experimental setup is given in Figure 2. A copper pipe has three regions as evaporator, adiabatic and condenser, power supply, electrical heater, flow meter, datalogger are the main components of the experimental setup. Details of the experimental apparatus were explained clearly in Gedik, (2016) [2]. Briefly, a copper pipe which has an inner and outer diameter of 18 and 19 mm respectively with a length of 100 mm was used as a thermosyphon. The working fluids were filled to cover one-third of the heat pipe volume (Jiao et al., 2008 [39]; Menlik et al., 2015 [40]). The applied heat energy to the evaporator region via electrical heater has been drawn by a cooling water circuit in the condenser region of TPCT. In the experiments, the distribution of TPCT surface temperature, inlet/outlet temperatures of the cooling water is measured for various heating power input, inclination angles and flow rates. The governing parameters are the heating power inputs changing 200 to 600 W, heat pipe inclination angle changing 30 to 90°, cooling water flow rates changing 10 to 30 L/h and type of working fluid.

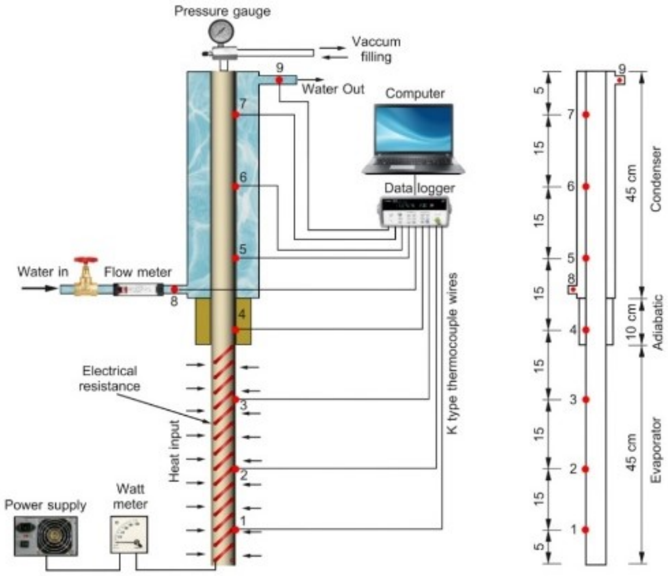

Figure 2. Schematic diagram of the experimental setup [1].

The thermal efficiency of the thermosyphon was calculated using the measurement data obtained from the experiments. The heat load drawn by the condenser region is calculated by the following equation.

$$\dot{Q}_C = m_w C_p \Delta T = m_w C_p (T_{w,o} - T_{w,i}) \tag{1}$$

Experimental efficiency of the TPCT is calculated as follow:

$$\eta = \frac{\dot{Q}_C}{\dot{Q}_E} \tag{2}$$

2.2. Artificial Neural Network (ANN)

The connection between the inputs and outputs can be represented more easily for the networks with bias than non-bias (Kurt & Kayfeci 2009 [26]). The calculation of the weighted sum of the input components/parameters is computed with the help of the Eq.3 given below.

$$NET_j = \sum_{i=1}^{n} w_{ij} x_i + b_i \tag{3}$$

The sigmoid function described in (Towards Data Science, 2019 [41]) is often used in machine learning algorithms, particularly in the testing of artificial neural networks, as a way of understanding the output of a node or "neuron". With the aid of sigmoid function the output of the jth neuron can be expressed as:

$$out_j = f\left(NET_j\right) = \frac{1}{1 + \exp\left(-kNET_j\right)} \tag{4}$$

The aim of the studied ANN model in this study is to estimate the thermal efficiency of TPCT depend on the fluid type, inclination angle, heating power and cooling flow rate. From the experimental measured and computed data were used the training of ANN model. For the training process, Backpropagation algorithm was used in this ANN model because of its popular and wide usage in many applications. The BP learning algorithm having three layers (input, output and hidden) was used in feed-forward. MATLAB software was used for the ANN model. The structure of ANN model is shown in Figure 3. In this structure, the type of working fluid, heating power, inclination angle and cooling water flow rate were used as four input variables. The efficiency of the TPCT was defined as the output variable. An optimal number of neurons was tried to be found and nine neurons gave the best structure in the hidden layer. A total of 81 data measured in the experiments were used in the training and testing set of the ANN.

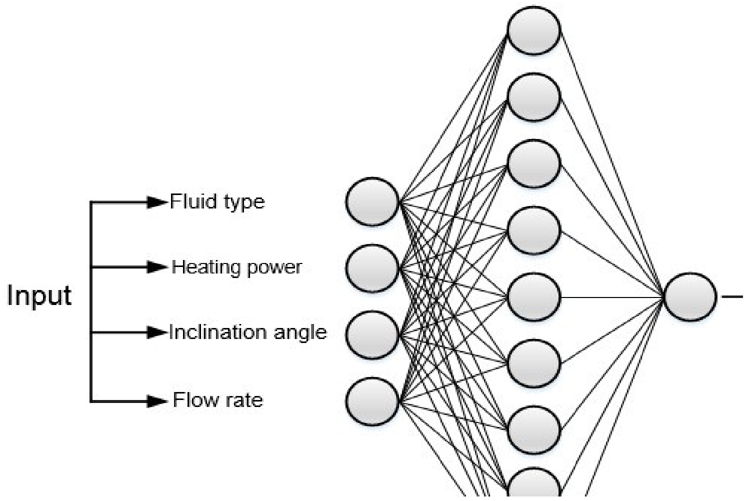

Figure 3. ANN structure.

In the proposed ANN model, the explicit formulation of efficiency (P) is achieved using the inputs, weights and normalization factors parameters. Trained ANN gives the all-necessary parameters. Inputs are multiplied by connection weights. Products and biases are summed, then transformed through a sigmoid function, (Eq.4) to produce an outcome with ease. In order to get the correct result from the formula proposed in this study, the normalization values given in Table 1 should be considered. The main purpose is to obtain the P in a functional form in terms of Ft, W, A, Q given as follows in Eq. 8-17.

$$P = \frac{1}{1 + e^{-\left(\frac{2.4309}{1+e^{-F1}} + \frac{7.0532}{1+e^{-F2}} - \frac{7.7829}{1+e^{-F3}} - \frac{6.4999}{1+e^{-F4}} + \frac{1.3784}{1+e^{-F5}} - \frac{1.1054}{1+e^{-F6}} - \frac{7.4239}{1+e^{-F7}} + \frac{10.6885}{1+e^{-F8}} + \frac{1.4595}{1+e^{-F9}} + 1.9681\right)}} \tag{5}$$

$$F1 = (0.7440\,Ft + 3.0693\,W + 3.2680\,A - 7.5662Q + 2.7498) \tag{6}$$
$$F2 = (16.9860\,Ft - 8.5599\,W - 0.3819\,A - 7.2432Q - 6.1207) \tag{7}$$
$$F3 = (0.0631\,Ft + 1.3277\,W + 0.7072\,A - 11.7203Q + 8.7993) \tag{8}$$
$$F4 = (14.8774\,Ft - 7.1054\,W - 0.5382\,A - 11.5731Q - 3.5099) \tag{9}$$
$$F5 = (-10.5419\,Ft - 9.7838\,W + 3.3311A + 1.4977Q + 7.0678) \tag{10}$$
$$F6 = (3.0602Ft + 5.1213\,W - 12.2349A - 4.3206Q + 9.9171) \tag{11}$$
$$F7 = (20.8258Ft + 7.8311W - 1.1373\,A + 2.1602Q - 6.3479) \tag{12}$$
$$F8 = (13.6664Ft + 1.2110\,W - 0.6318\,A + 0.6215Q - 2.3536) \tag{13}$$
$$F9 = (-5.4369Ft - 1.5827\,W + 1.2731A - 24.6166Q + 17.4375) \tag{14}$$

Functions F1, F2, F3, F4, F5, F6, F7, F8 and F9 were obtained by employing independent variables from Equations 8-17. P was achieved by using functions from F1 to F9 in Equation 8.

Table 1. Normalization values of inputs and output

Fluid type	Heating power input	Inclination angle	Cooling water flow rate	Efficiency of the TPCT
(Ft)	(W)	(A)	(Q)	(P)
4	800	100	40	1

RMS, SSE and R2 which can be expressed in Eqs (18-20) were considered for estimation of the network's performance and t_j is the target value, o_j is the output value, p is the sample size. Computed these statistical parameters were given in Table 2.

$$RMS = \left((1/p) \sum_j \left(\left| t_j - o_j \right| \right)^2 \right)^{1/2} \tag{15}$$

$$SSE = \sum_j \left(\left| t_j - o_j \right| \right)^2 \tag{16}$$

$$R^2 = 1 - \left(\frac{\sum_j \left(t_j - o_j \right)^2}{\sum_j \left(o_j \right)^2} \right) \tag{17}$$

Table 2. Statistical parameters of the ANN

Parameters	Training	Test
MAPE (%)	1.31	3.06
RMS	0.0087	0.0221
SSE	0.0054	0.0049
R^2	0.9998	0.9989
cov	0.0146	0.0344

3. Results and discussions

The comparisons between real (target) and predicted (output) thermal efficiencies of TPCT are shown in Figure 4. A total of 71 data measured in the experiments were used in the training of the artificial neural network and the other 10 were randomly selected as test data. ANN training and test results are shown in Figure 4.

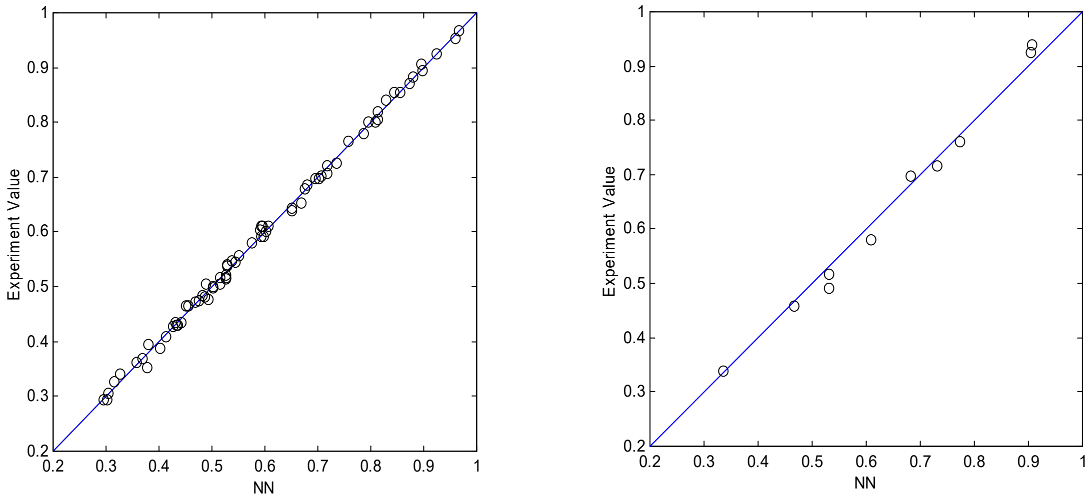

(a) (b)

Figure 4. Set performances a) training b) test

The results in Figure 4 show that the neural network is successful in learning the relationship between the output (thermal efficiency of TPCT) of various input parameters. Graphs of Figure 5 show the predicted thermal efficiency of TPCT obtained from ANN at varied values of input parameters such as heating power input, fluid type and cooling water flow rate.

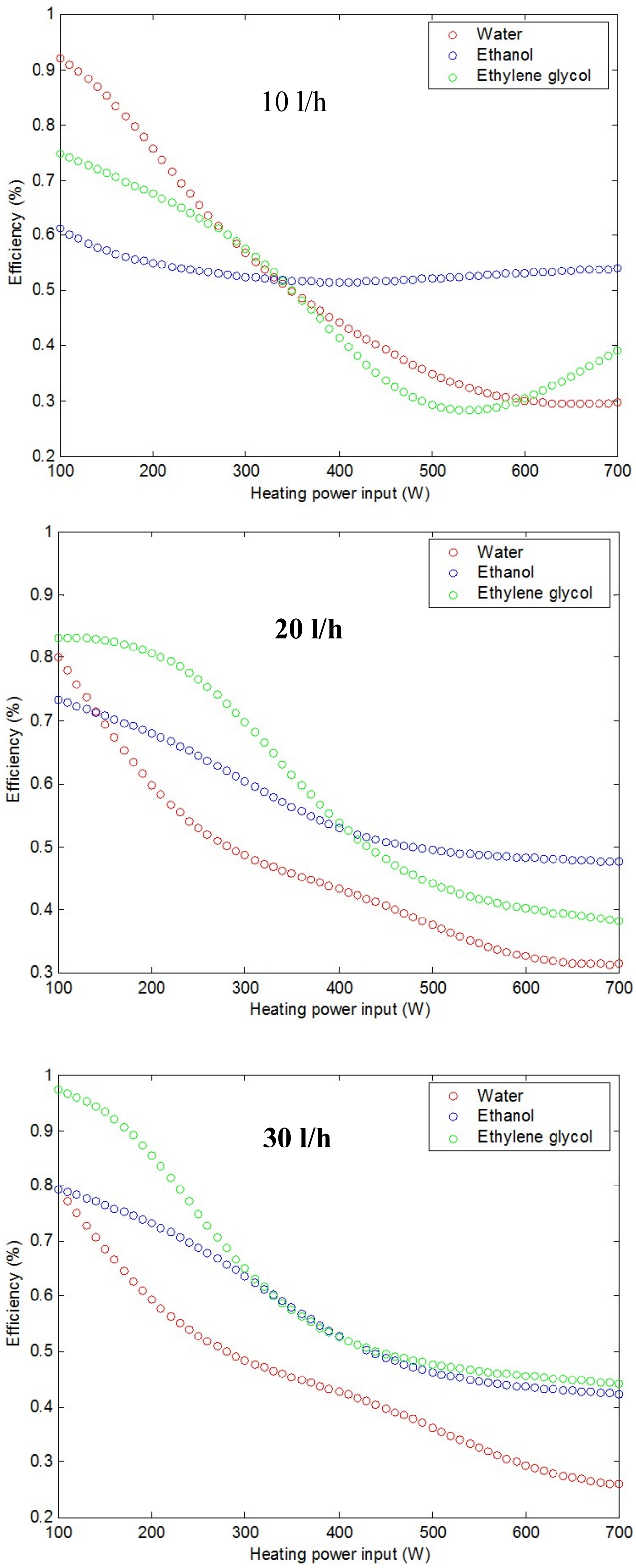

Figure 5. Variations of predicted TPCT efficiency by heating power input at 30° inclination angle

It is clear from the figure that when the heating power input has increased, thermal efficiency has decreased for all types of fluid and these decreases are much more with increasing cooling water flow rate.

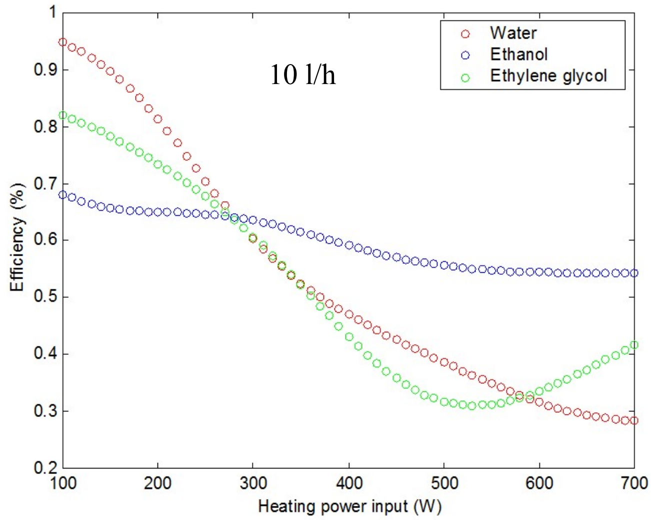

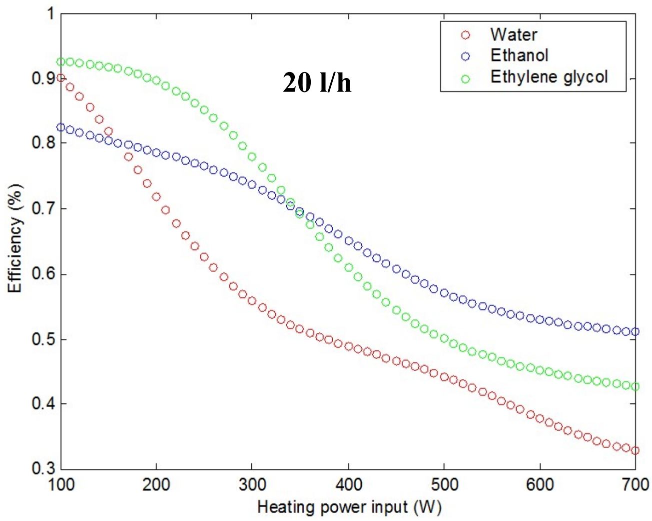

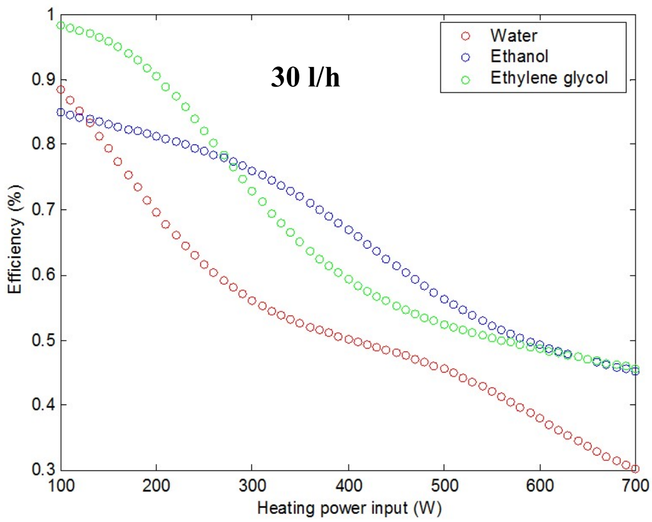

Figure 6. Variations of predicted TPCT efficiency by heating power input at 60° inclination angle.

In the case that the applied heating power is 100 W, the water is considered to be the best efficacious fluid for low cooling water flow rate and in high heating power, this situation was realized for ethanol working fluid.

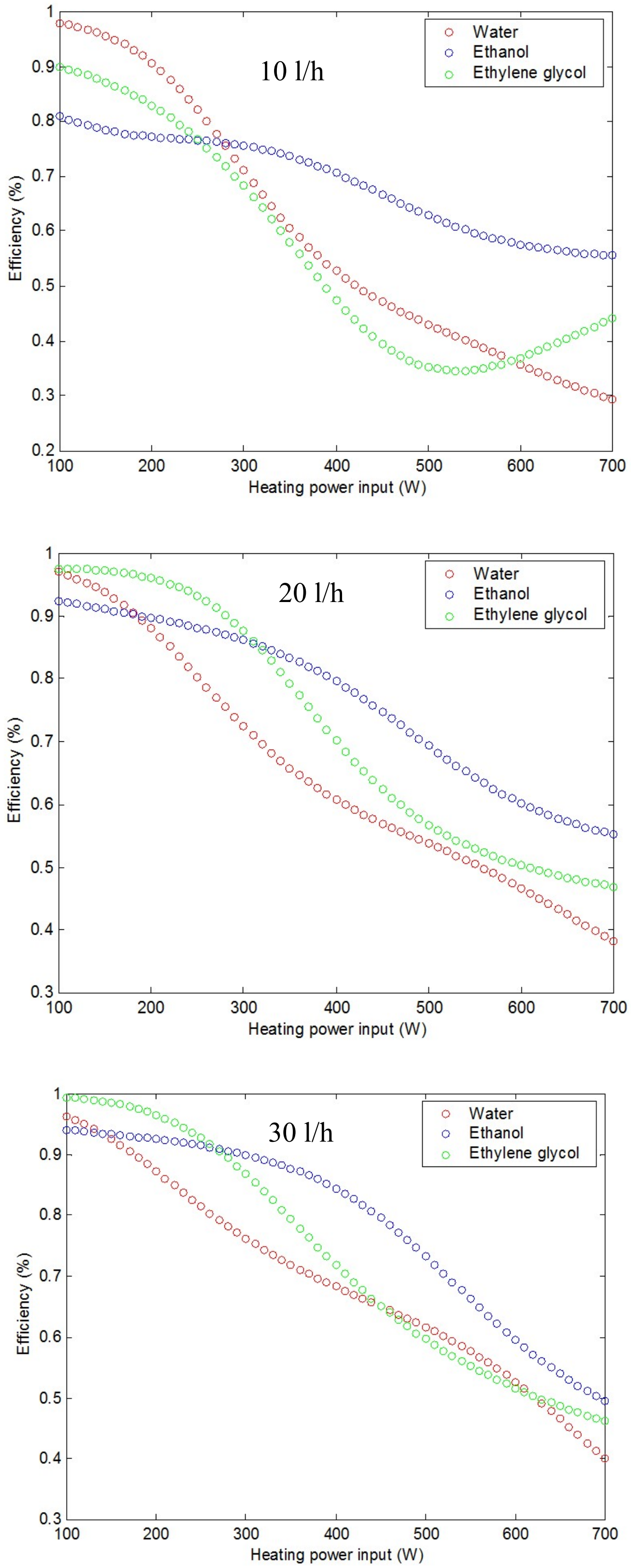

Figure 7. Variations of predicted TPCT efficiency by heating power input at 90° inclination angle.

When the graphs are examined, the increase in cooling water flow rate in the same heat load, generally, the efficiency of TPCT filled with water has decreased and the efficiency of TPCT filled with other working fluids (ethanol and ethylene glycol) has increased. Figures 6 and 7 show the variations of TPCT efficiency for the 60º and 90º inclination angle respectively considering the various ANN input parameters. It was found that at low heat load and low cooling water flow rate, water is the most efficient working fluid for all inclination angles.

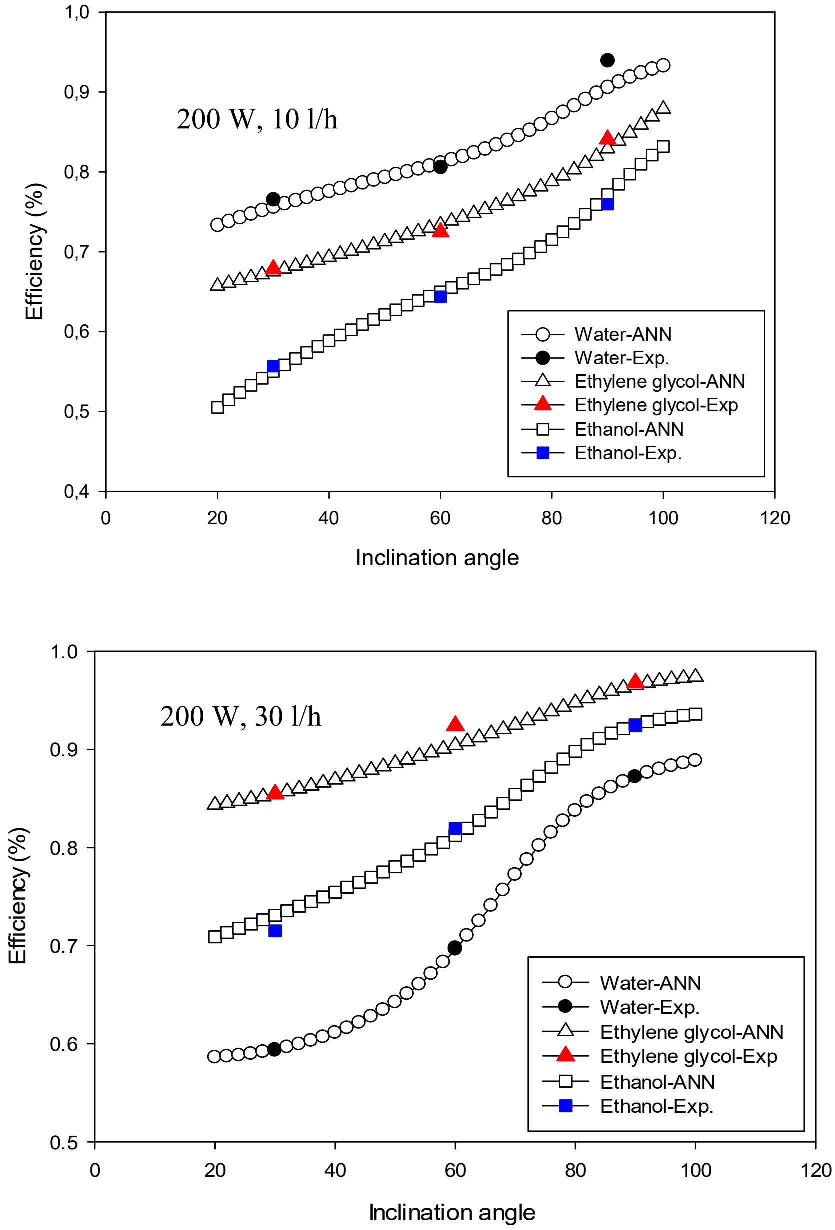

Figure 8. Comparison of efficiency values obtained from ANN model and experimental study

For the situation of low heat load and high flow rate of the coolant ethylene glycol working fluid was found more efficient whereas ethanol is best at high heat load for all inclination angle. In the same values of heating power input and flow rate of coolant, ethanol and ethylene glycol showed similar properties as working fluids; those efficiency values for the 30° inclination angle were estimated at 60% and 75%, respectively whereas it was predicted as 68% and 82%, 81% and 90% for 60° and 90° inclination angles respectively. Increasing inclination angle has caused to increase TPCT efficiency for all working fluid types. At low heating power input, water is more efficient, whereas ethanol is more efficient at high heating power input. At the same heating power input, an increase in the flow rate of the cooling water decreased some efficiency values and increased others. This situation has been explained in Gedik, (2016) [2]. A 100% increase in the flow rate sometimes causes higher temperature differences up to 100% and consequently a tendency to increase or decrease the efficiency values of TPCT depending on the flow rate. Sözen et al. (2016) [22] indicated that efficiency values decreased as the flow rate increased. Besides that, according to the results obtained, the highest temperature difference was obtained in the cooling water at the condenser zone for working fluid ethylene glycol at low heating power input and high cooling water flow rates. However, at higher heating power inputs, the efficiency of the TPCT, whose working fluid was ethanol, was greater. Experimental and ANN results of TPCT efficiency for different working fluids, cooling water flow rates, inclination angle at 200 W heating power input are given in Figure 8. It can be understood that the increase in the inclination angle causes an increase in the efficiency of the TPCT. For instance; the efficiency value of TPCT that had been about 75% at an inclination angle of 30° for water as a working fluid, has approximately been 80% and 93% at situations in which inclination angle had been 60° and 90° respectively. A similar situation is also valid for other working fluids. Both in ANN and experimental study, maximum efficiency value was found when working fluid is water for the highest inclination angle at 10 L/h cooling water flow rate.

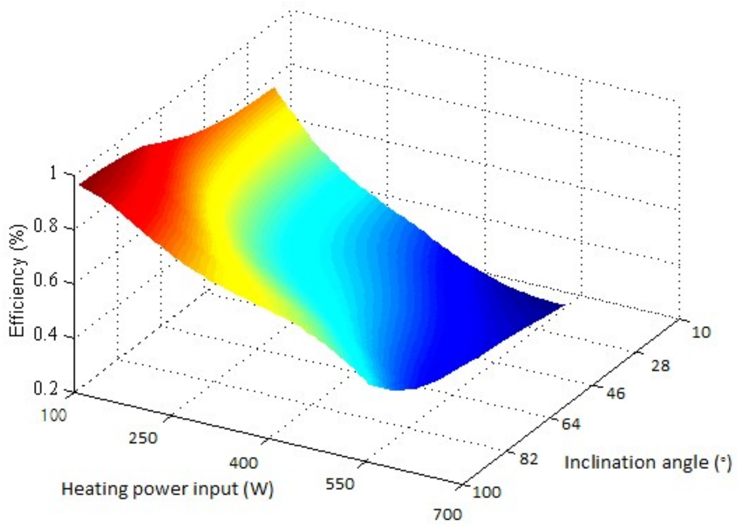

Figure 9. The 3D plots of TPCT efficiency for water

The results of the ANN and the experimental results are in good agreement with each other. Also; the increase in cooling water flow rate has changed the efficiency values of the working fluids. For 10 L/h cooling water flow rate, the water has performed the best efficiency; at high cooling water flow rate (30 L/h), on the other hand, ethylene glycol has performed a better efficiency. As the angle of inclination increases, the phase change event (condensation and evaporation) in the thermosyphon occurs faster because of gravity. For this reason, the efficiency of the TPCT at a 90° inclination angle in the vertical position was higher. Figure 9 is shown for water and a flow rate of 30 L/h for a better understanding of the effect of the heating power input and the inclination angle on the thermal efficiency of the TPCT. As can be understood from the three-dimensional surface graph, the efficiency of TPCT is a function of inclination angles. It is also an opposite function of the heating power input.

4. Conclusions

An experimental study and ANN approach have been conducted in the present study to examine the thermal efficiency of TPCT under various parameters effect, i.e., (i) heating power input, (ii) inclination angle, (iii) cooling water flow rate, and (iv) type of working fluids. The ANN model using BP learning algorithm was successfully used to predict the complex nonlinear relationship between the thermal efficiency and input variables of TPCT. The data obtained from ANN were represented in graphs and discussed in detail. The concluding remarks are:

- The comparisons between the predicted data and experimental data proved ANN model have the capability of recognizing the relationship between input and output events. Predicted thermal efficiency values were found to be in excellent agreement with the corresponding experimental data.
- The increase in the inclination angle increased the TPCT efficiency while the increase in heating power input decreased efficiency.
- For low cooling water flow rates (10 L/h ≤), water was more effective in terms of the thermal efficiency of TPCT, whereas for higher flow rates (30 L/h≥) ethylene glycol was a more effective working fluid.
- ANN is a useful tool to predict the thermal efficiency of TPCT. The methodology proposed in this study can be used very easily for such kind of heat transfer application.

Nomenclature

bi	: bias
c_p	: specific heat [J/kgK]
MAPE	: mean absolute percentage error
$\dot{m}$	: mass flow rate (kg/s)
NET_j	: weighted sum of the jth neuron
out_j	: output of the jth neuron.
$\dot{Q}_C$	: heat transfer rate of condenser (kW)
$\dot{Q}_E$	: heat transfer rate of condenser (kW)
RMS	: root mean squared
R2	: statistical coefficient
SSE	: sum of squared error
t	: target
T	: temperature [K]
w_{ij}	: weighted between the jth neuron and the ith neuron.
X_i	: input of the ith neuron.
Subscripts	
o/out	: outlet
p	: pattern size
P	: efficiency (ANN)
in	: inlet
Greek letters	
η	: efficiency (experimental)

References

[1] Gedik, E. (2016). Experimental investigation of the thermal performance of atwo-phase closed thermosyphon at different operating conditions. Energy and Buildings, 127, 1096-1107. https://doi.org/10.1016/j.enbuild.2016.06.066.

[2] Gedik, E., Yılmaz, M., & Kurt, H. (2016). Experimental investigation on the thermal performance of heat recovery system with gravity assisted heat pipe charged with R134a and R410A. Applied Thermal Engineering, 99, 334-342. https://doi.org/10.1016/j.applthermaleng.2015.12.075.

[3] Andrzejczyk, R. (2019). Experimental Investigation of the Thermal Performance of a Wickless Heat Pipe Operating with Different Fluids: Water, Ethanol, and SES36. Analysis of Influences of Instability Processes at Working Operation Parameters. Energies, 12,80 1-28. https://doi.org/10.3390/en12010080.

[4] Sarafraz, M.M., Tian, Z., Tlili, I., Kazi, S., Goodarzi, M. (2020). Thermal evaluation of a heat pipe working with n-pentane-acetone and n-pentane-methanol binary mixtures. Journal of Thermal Analysis and Calorimetry, 139, 2435-2445. https://doi.org/10.1007/s10973-019-08414-2.

[5] Faghri, A. (1995). *Heat Pipe Science and Technology*. Taylor & Francis.

[6] Fadhl, B., Wrobel, L.C., & Jouhara H. (2013). Numerical modelling of the temperature distribution in a two-phase closed thermosyphon. Applied Thermal Engineering, 60, 122-131. https://doi.org/10.1016/j.applthermaleng.2013.06.044.

[7] Kerrigan, K., Jouhara, H., O'Donnell, G.E., Robinson, A.J. (2011). Heat pipe-based radiator for low grade geothermal energy conversion in domestic space heating. Simulation Modelling Practice and Theory, 19, 1154-1163. https://doi.org/10.1016/j.simpat.2010.05.020.

[8] Fadhl, B., Wrobel, L.C., & Jouhara, H. (2015). CFD modelling of a two-phase closed thermosyphon charged with R134a and R404a. Applied Thermal Engineering, 78, 482-490. https://doi.org/10.1016/j.applthermaleng.2014.12.062.

[9] Farsi, H., Joly, J.L., Miscevic, M., Platel, V., & Mazet, N. (2003). An experimental and theoretical investigation of the transient behavior of a two-phase closed thermosyphon. Applied Thermal Engineering, 23,1895-1912. https://doi.org/10.1016/S1359-4311(03)00147-9.

[10] Kamyar, A., Ong, K.S., & Saidur, R. (2013). Effects of nanofluids on heat transfer characteristics of a two-phase closed thermosyphon. International Journal of Heat and Mass Transfer, 65, 610-618. https://doi.org/10.1016/j.ijheatmasstransfer.2013.06.046.

[11] Jafari, D., Filippeschi, S., Franco, A., Marco, P.D. (2017). Unsteady experimental and numerical analysis of a two-phase closed thermosyphon at different filling ratios. Experimental Thermal and Fluid Science, 81, 164-174. https://doi.org/10.1016/j.expthermflusci.2016.10.022.

[12] Jafari, D., Franco, A., Filippeschi, S., Marco, P.D. (2016). Two-phase closed thermosyphons: A review of studies and solar applications. Renewable and Sustainable Energy Reviews. 2016;53:575-593. https://doi.org/10.1016/j.rser.2015.09.002.

[13] Ma, L., Shang, L., Zhong, D., & Ji, Z. (2017). Experimental investigation of a two-phase closed thermosyphon charged with hydrocarbon and Freon refrigerants. Applied Energy, 207, 665-673. https://doi.org/10.1016/j.apenergy.2017.06.100.

[14] Naresh, Y., & Balaji C. (2018). Thermal performance of an internally finned two phase closed thermosyphon with refrigerant R134a: A combined experimental and numerical study. International Journal of Thermal Science, 126, 281-293. https://doi.org/10.1016/j.ijthermalsci.2017.11.033.

[15] Huminic, G. & Huminic, A. (2011). Heat transfer characteristics of a two-phase closed thermosyphons using nanofluids. Experimental Thermal and Fluid Science, 35, 550-557. https://doi.org/10.1016/j.expthermflusci.2010.12.009.

[16] Kannan, M., Senthil, R., Baskaran, R., Deepanraj, B. (2014). An experimental study on heat transport capability of a two phase thermosyphon charged with different working fluids. American Journal of Applied Sciences, 1, 584-591. https://doi.org/10.3844/ajassp.2014.584.591.

[17] Noie, S.H., Emami, M.R.S., & Khoshnoodi, M. (2007). Effect of inclination angle and filling ratio on thermal performance of a two-phase closed thermosyphon under normal operating conditions. Heat Transfer Engineering, 28, 365-371. https://doi.org/10.1080/01457630601122997.

[18] Ong, K.S., Haider, M.D., & Alalhi, E. (1999). Experimental investigation on hysteresis effect in vertical two phase closed thermosyphons. Applied Thermal Engineering, 19, 399-408. https://doi.org/10.1016/S1359-4311(98)00051-9.

[19] Park, Y.J, Kang, H.K., & Kim, C.J. (2002). Heat transfer characteristics of a two-phase closed thermosyphon to fill charge ratio. International Journal of Heat and Mass Transfer, 45, 4655-4661. https://doi.org/10.1016/S0017-9310(02)00169-2.

[20] Shabgard, H., Xiao, B., Faghri, A., Gupta, R., & Weissman, W. (2014). Thermal characteristics of a closed thermosyphon under various filling conditions. International Journal of Heat and Mass Transfer, 70, 91-102. https://doi.org/10.1016/j.ijheatmasstransfer.2013.10.053.

[21] Payakaruk, T., Terdtoon, P., & Ritthidech, S. (2000). Correlations to predict heat transfer characteristics of an inclined closed two-phase thermosyphon at normal operating conditions. Applied Thermal Engineering, 20, 781-790. https://doi.org/10.1016/S1359-4311(99)00047-2.

[22] Sözen, A., Menlik, T., Gürü, M., Boran, K., Kılıç, F., Aktaş, M., & Çakır, M.T. (2016). A comparative investigation on the effect of fly-ash and alumina nanofluids on the thermal performance of two-phase closed thermo-syphon heat pipes. Applied Thermal Engineering, 96, 330-337. https://doi.org/10.1016/j.applthermaleng.2015.11.038.

[23] Boostani, M., Karimi, H., & Azizi, S. (2017). Heat transfer to oil-water flow in horizontal and inclined pipes: Experimental investigation and ANN modeling. International Journal of Thermal Science, 111, 340-350. https://doi.org/10.1016/j.ijthermalsci.2016.09.005.

[24] Kalogirou, S.A. (2001). Artificial neural networks in the renewable energy systems applications: a review. Renewable and Sustainable Energy Reviews, 5, 373-401. https://doi.org/10.1016/S1364-0321(01)00006-5.

[25] Kurt, H., Atik, K., Ozkaymak, M., Binark, A.K. (2006). The artificial neural networks approach for evaluation of temperature and density profiles of salt gradient solar pond. Journal of Energy Institute, 80, 46-51. https://doi.org/10.1179/174602207X171570.

[26] Kurt, H., & Kayfeci, M. (2009). Prediction of thermal conductivity of ethylene glycol–water solutions by using artificial neural networks. Applied Energy, 86, 2244-2248. https://doi.org/10.1016/j.apenergy.2008.12.020.

[27] Sarle, W.S. (1994). Neural Networks and Statistical Models. Proceedings of the Nineteenth Annual SAS Users Group International Conference, Cary, NC: SAS Institute, USA, 1538-1550.

[28] Chaloulakou, A., Saisana, M., & Spyrellis, N. (2003). Comparative assessment of neural networks and regression models for forecasting summertime ozone in Athens. Science of the Total Environment, 313, 1-13. https://doi.org/10.1016/S0048-9697(03)00335-8.

[29] Fichera, A., & Pagano, A. (2002). Neural network-based prediction of the oscillating behaviour of a closed loop thermosyphon. International Journal of Heat and Mass Transfer, 45, 3875-3884. https://doi.org/10.1016/S0017-9310(02)00095-9.

[30] Sanaye, S., & Hajabdollahi, H. (2010). Thermal-economic multi-objective optimization of plate fin heat exchanger using genetic algorithm. Applied Energy, 87, 1893-1902. https://doi.org/10.1016/j.apenergy.2009.11.016.

[31] Caner, M., Gedik, E., & Keçebas, A. (2011). Investigation on thermal performance calculation of two type solar air collectors using artificial neural network. Expert Systems With Applications, 38, 1668-1674. https://doi.org/10.1016/j.eswa.2010.07.090.

[32] Ceylan, İ., Gedik, E., Erkaymaz, O., & Gürel, A.E. (2014). The artificial neural network model to estimate the photovoltaic modul efficiency for all regions of the Turkey. Energy and Building, 84, 258-267. https://doi.org/10.1016/j.enbuild.2014.08.003.

[33] Akdag, U., Komur, M.A., & Ozguc F. (2009). Estimation of heat transfer in oscillating annular flow using artifical neural networks. Advances in Engineering Software, 40, 864-870. https://doi.org/10.1016/j.advengsoft.2009.01.010.

[34] Shanbedi, M., Amiri, A., Rashidi, S., Heris, S.Z., & Baniadam, M. (2015). Thermal Performance Prediction of Two-Phase Closed Thermosyphon Using Adaptive Neuro- Fuzzy Inference System. Heat Transfer Engineering, 36, 315-324. https://doi.org/10.1080/01457632.2014.916161.

[35] Shanbedi, M., Jafari, D., Amiri, A., Heris, S.Z., & Baniadam, M. (2013). Prediction of temperature performance of a two-phase closed thermosyphon using Artificial Neural Network. Heat and Mass Transfer, 49, 65-73. https://doi.org/10.1007/s00231-012-1066-y.

[36] Komeilibirjandi, A., Raffiee, A.H., Maleki, A., Nazari, M.A., Shadloo, M.S. (2020). Thermal conductivity prediction of nanofluids containing CuO nanoparticles by using correlation and artificial neural network. Journal of Thermal Analysis and Calorimetry, 139, 2679-2689. https://doi.org/10.1007/s10973-019-08838-w.

[37] Sadrameli, S.M., Forootan, D., & Farajimoghaddam, F. (2020). Effect of working fluid inventory and heat input on transient and steady state behavior of a thermosyphon. Journal of Therm Analysis and Calorimetry, https://doi.org/10.1007/s10973-020-09294-7.

[38] Senthilkumar, C., Krishnan, A.S., & Solomon, A.B. (2020). Effect of thin porous copper coating on the performance of wickless heat pipe with R134a as working fluid. Journal of Thermal Analysis and Calorimetry, 139, 963-973. https://doi.org/10.1007/s10973-019-08176-x.

[39] Jiao, B., Qiu, L.M., Zhang, X.B., & Zhang, Y. (2008). Investigation on the effect of filling ratio on the steady-state heat transfer performance of a vertical two-phase closed thermosyphon. Applied Thermal Engineering, 28: 1417-1426. https://doi.org/10.1016/j.applthermaleng.2007.09.009.

[40] Menlik, T., Sozen, A., Gürü, M., & Oztas, S. (2015). Heat transfer enhancement using MgO/water nanofluid in heat pipe. Journal of the Energy Institute, 88, 247-257. https://doi.org/10.1016/j.joei.2014.10.001.

[41] Towards Data Science. (2019). Sigmoid neuron-building block of deep neural networks. Retrieved from https://towardsdatascience.com/sigmoid-neuron-deep-neural-networks-a4cd35b629d7. Accessed June 1, 2020.